J Mater Sci (2008) 43:6182–6192
DOI 10.1007/s10853-008-2932-3

Evaluation of additive effects and homogeneity of the starting mixture on the nuclei-growth processes of barium titanate via a solid state route

Chie Ando · Toshimasa Suzuki · Youichi Mizuno · Hiroshi Kishi · Sayuri Nakayama · Mamoru Senna

Received: 26 December 2007 / Accepted: 5 August 2008 / Published online: 26 August 2008

Abstract In an attempt to obtain finest possible microparticles of $BaTiO_3$ (BT) with highest possible tetragonality via a solid state route, starting mixtures comprising $BaCO_3$ and TiO_2 were subjected to various pretreatments including addition of glycine and mechanical activation. Reaction processes were monitored by the changes in the weight, crystallinity, and morphology in detail. While mechanical activation with glycine significantly increased the rate of reaction and homogeneity of the particle size of the product, BT, simultaneous particle growth of BT was intolerably acute for micro-electronic devices. The fast particle coarsening was predominated by the coalescence of BT tiny particles formed around titania. A mixture with higher homogeneity was attained by using finer starting materials under wet mixing, avoiding significant mechanical stressing. Particle growth of BT was suppressed to ca. 100 nm to obtain fully crystallized BT particles without significant loss of tetragonality and, hence, close to meet our requirements for MLCCs.

C. Ando (✉) · T. Suzuki · Y. Mizuno · H. Kishi
Material Development Department, Taiyo Yuden Co., Ltd., 5607-2 Nakamuroda-machi, Takasaki-shi, Gunma 370-3347, Japan
e-mail: cando@jty.yuden.co.jp

S. Nakayama · M. Senna
Technofarm AXESZ Co., Ltd., 3-45-4 Kami-ishihara, Choufu, Tokyo 182-0035, Japan

M. Senna
Faculty of Science and Technology, Keio University, 3-14-1 Hiyoshi, Kohoku-ku, Yokohama 223-8522, Japan

Introduction

To realize miniaturization and higher capacitance of multi-layer ceramic capacitors (MLCCs), $BaTiO_3$ (BT) powders with well-dispersed small grains, narrow particle size distribution, and higher crystallinity and consequent higher tetragonality are required. Particle size less than 100 nm is highly desirable as the active layer thickness of MLCCs goes down to less than 1 μm [1]. At the same time, a well-known decrease of tetragonality with reducing the BT particle size [1, 2] should be avoided. It is commonly believed that BT particles obtained from wet chemical methods such as hydrothermal or sol–gel processes are superior to those from solid state reaction [3–5]. This is actually not always the case. A solid state route has been progressed considerably with the advent of purer and finer starting materials at a reasonable price [6, 7]. After we have published several works along this line [8–12], we here further challenge improving solid state processes.

Mechanisms of the solid state reaction toward BT are well documented [13–17]. Lotnyk et al. [16, 17] verified a direct reaction between TiO_2 and $BaCO_3$ by analyzing the orientation of produced BT particles formed between a single crystalline TiO_2 thin film and $BaCO_3$ just deposited on the titania film. They further showed absence of the second phase, Ba_2TiO_4 (B2T), because of the role of BT nuclei serving as a barrier of B2T formation. Direct reaction between $BaCO_3$ and TiO_2 particles was also reported [8] where Ba^{2+} ions diffuse into TiO_2 particles in an ambient atmosphere [8].

For a faster reaction at lower temperatures, larger number of contact points between $BaCO_3$ and TiO_2 and shorter diffusion path for Ba^{2+} ion species are decisive. Therefore, we pay attention to obtain reaction mixtures of fine $BaCO_3$ and

TiO_2 particles with highest possible homogeneity. For these purposes, we conventionally disperse ceramic powders in a ball mill or by a media agitation mill. Intensive mechanical stressing induces mechanochemical effects [18], which are usually effective to decrease temperatures of reaction initiation and termination. Another aspects we are interested in are organic additives such as amino acid and polyamide, which we previously found to accelerate decomposition of barium carbonate and, hence, to initiate Ba^{2+} diffusion at lower temperatures [11, 12, 19]. We also reported on the formation of fine and well-crystallized BT particles with high tetragonality by dry milling the starting mixture with organic additives [11].

Although there is a common understanding in the literature cited above that low-temperature synthesis is favorable for finer particles, no straightforward information is available how to make the sharp particle size distribution and high tetragonality compatible. We therefore try to prepare in this study three different starting mixtures with widest possible variation of their reactivity and compare their reaction processes including growths of crystals and particles, in order to avail ourselves the compatibility mentioned above. More specifically, a standard, physical mixture was mechanically activated intensively with an additive, glycine, and compared with an intact mixture. For mechanical activation, we used a planetary mill, which was capable to give mechanical energy higher than those with a vibration mill used in our previous studies [8, 9, 11]. Furthermore, we also prepared an intimately homogenized mixture from much finer starting materials.

Table 1 Properties of starting materials

Sample	SBET (m^2/g)	Particle size from SBET (nm)	Rutil (%)
S (SG)			
$BaCO_3$	11	127	–
TiO_2	30	49	38
FB			
$BaCO_3$	36	39	–
TiO_2	150	10	2

	Impurities (%)						
	Fe_2O_3	Al_2O_3	SiO_2	Na_2O	SrO	CaO	Cl
S (SG)							
$BaCO_3$	0.001	–	–	0.003	0.006	0.000	0.006
TiO_2	0.002	0.003	0.000	0.000	–	–	0.004
FB							
$BaCO_3$	0.000	–	–	0.000	0.007	0.000	0.002
TiO_2	0.001	0.002	0.010	0.002	–	–	0.010

Experimental

We started from highly pure fine particles of $BaCO_3$ and TiO_2 for electroceramics. Their properties and transmission electron micrographs are given in Table 1 and Fig. 1,

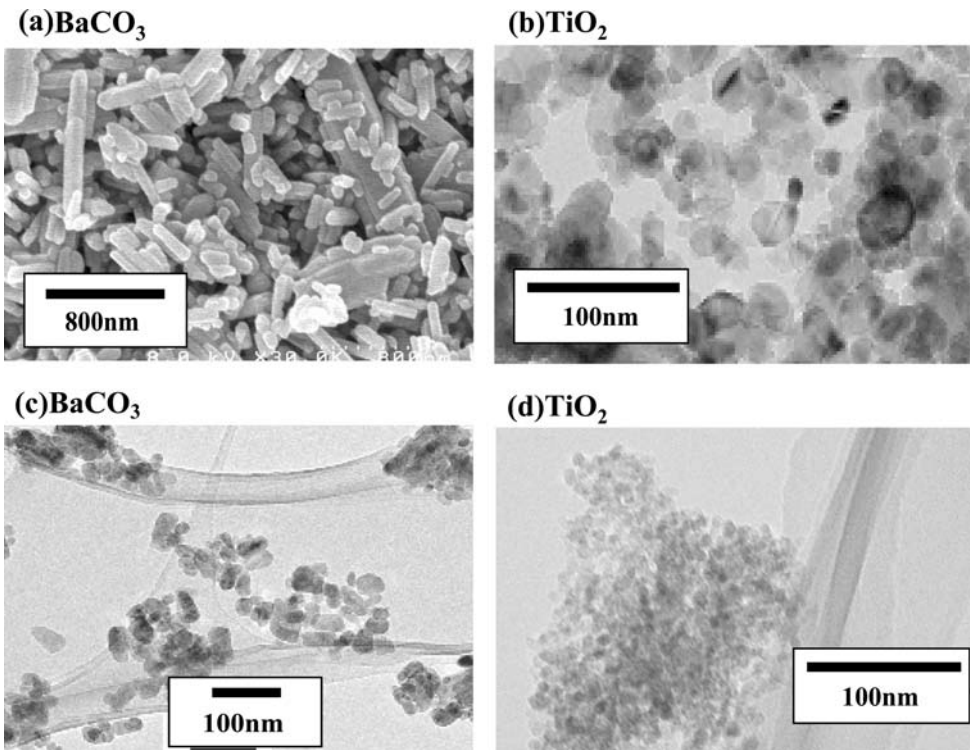

Fig. 1 (**a**, **b**) SEM and TEM micrographs of starting materials of sample S (SG). (**c**, **d**) TEM micrographs of starting materials of sample FB

respectively. $BaCO_3$ (Fig. 1a) and TiO_2 (Fig. 1b) were mixed in the molar ratio 1:1 and pre-dispersed to obtain aqueous slurry. The slurry was homogenized in a rotary pot mill at 130 rpm for 20 h with 1.5 mm yttrium-stabilized zirconia ball and dried to obtain sample S. We added 1.5% glycine to sample S and mixed in a planetary mill (Pulversitte 5, Fritsch) at rotation and revolution speeds 245 and 196 rpm, respectively, for 1 h with a PTFE vessel and nylon-coated steel balls of 10 mm of diameter to obtain sample SG.

As an alternative starting mixture under suppressed mechanical energy during milling, we prepared sample FB by using ultra-fine starting materials shown in Fig. 1c and d. They were mixed in an equimolar ratio and dispersed with a rotary pot mill at 100 rpm for 90 h using the polyethylene pot and yttrium-stabilized zirconia ball of 0.5 mm of diameter in distilled water to obtain sample FB after freeze-drying the slurry. We have analyzed the molar ratio, Ba/Ti, to be 0.999 (±0.001) for all the three samples by means of X-ray fluorescent analysis.

Size and morphology of the particles were determined by scanning transmission electron microscopy (STEM: JEM-3000F, JEOL) and scanning electron microscopy (SEM: S-4500, Hitachi). The particle size was estimated as a Feret diameter [20]. Particle size distribution was determined from image analysis of more than 300 particles. The average slope, M, of the cumulative distribution curve between 20 and 80% was adopted as the measure of the sharpness of the particle size distribution [8]. A larger M value means a narrower particle size distribution. Mixing homogeneity of $BaCO_3$ and TiO_2 was evaluated from the back-scattered electron (BSE) micrographs on the surface of the sample compressed at 0.5 GPa by using the same SEM given above.

Reaction kinetic processes were primarily monitored by thermo-gravimetrical analysis (TGA: Thermoplus, Rigaku) up to 1000 °C at the constant rate of heating, 5 °C/min, under 150 mL/min air flow. We chose two heating programs, i.e. (i) to air quench after heating at 5 °C/min up to 700 or 790 °C and (ii) to slow cool at 5 °C/min after keeping at 860 or 880 °C for 4 h. Crystallographical analysis was carried out by conventional powder X-ray diffractometry (XRD, CuKα radiation, RINT, Rigaku). Tetragonality was determined from XRD after refining by Rietveld analysis using Rietan-2000 [21].

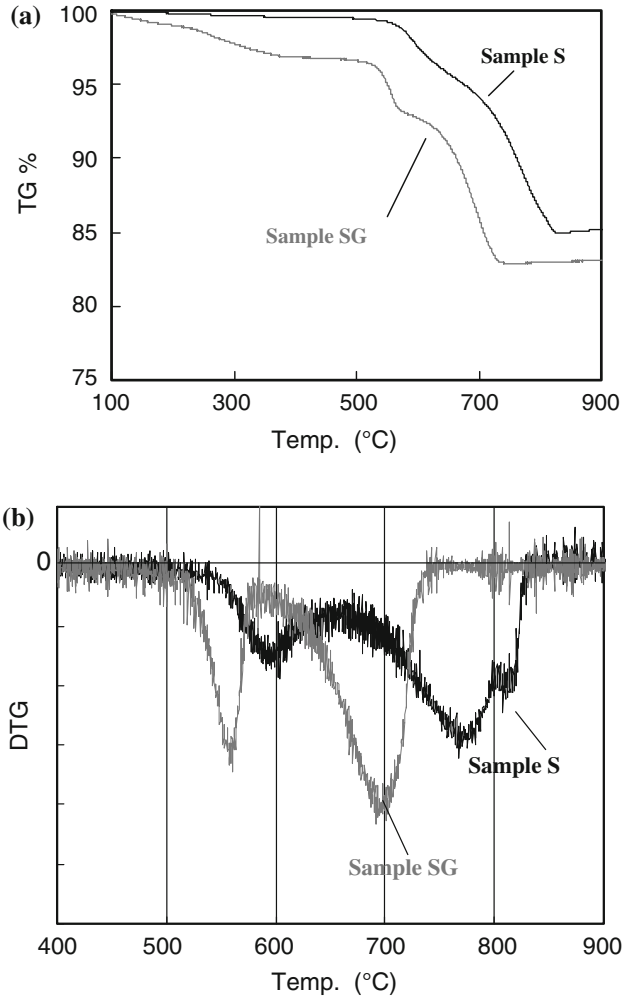

Fig. 2 TG (**a**) and DTG (**b**) profiles of the samples S and SG

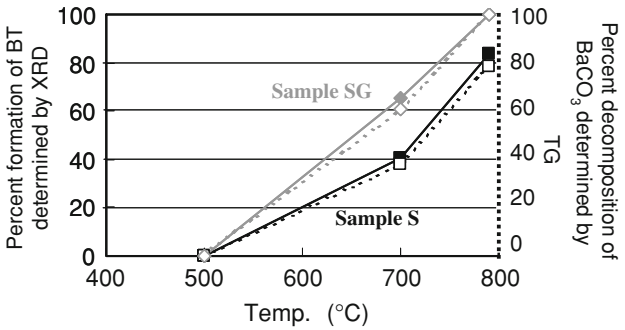

Fig. 3 Change in the percent formation of BT determined by XRD and percent decomposition of $BaCO_3$ determined by TG with calcination temperature

Experimental results

Thermal behaviors of samples S and SG

Figure 2 shows thermogravimetric (TG) and their derivative profiles, i.e. differential thermogravimetry (DTG) of samples S and SG. The weight loss at around 300 °C exhibits decomposition of organic additives, including abraded fluororesin and nylon, while those above 400 °C to the decomposition of $BaCO_3$. The reaction between $BaCO_3$ and TiO_2 comprises two distinct stages, i.e. the stage of BT formation at $BaCO_3$ and TiO_2 contact points, followed by

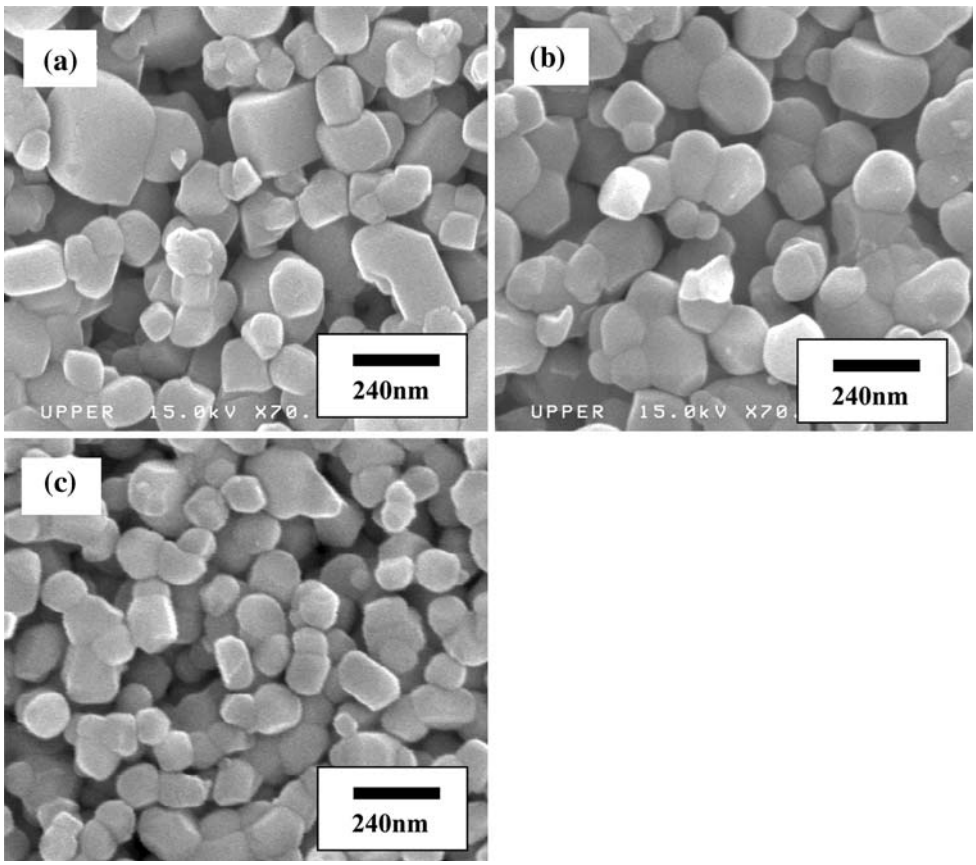

Fig. 4 SEM micrographs of BT calcined at 880 °C: (**a**) sample S, (**b**) sample SG, and (**c**) sample FB

Table 2 Average particle size and tetragonality of BT calcined at 880 °C

Sample	Average particle size (nm)	Slope: *M* value	SBET (m^2/g)	Particle size from SBET (nm)	Tetragonality, c/a
S	127	4.3	5.6	178	1.0085
SG	145	5.6	4.8	207	1.0075
FB	121	5.5	7.2	139	1.0082

the second stage, i.e. diffusion of Ba^{2+} toward TiO_2 through BT product [8]. Sample SG shows a larger portion of the first stage. Sample SG terminates the reaction at lower temperatures than sample S. The termination temperature of sample SG is lower by 50 °C than the sample milled by a vibration mill for 5 h, or by 70 °C than the sample milled with glycine and milled for 3 h [8, 11]. An increase in the reactivity of $BaCO_3$ and TiO_2 by a synergetic effect of glycine and mechanical activation is thus appreciable.

Progress of the solid state reaction toward BT was monitored by TG (dashed lines) and XRD (solid lines) in Fig. 3. Both values are very close to each other. This tallies well with the statements of Lotnyk et al. [16, 17] or Buscaglia et al. [7] in the sense that $BaCO_3$ and TiO_2 react directly at temperatures below 800 °C in air. We did not observe coexistence of second phases like B2T.

Morphological properties of the powder samples

Figure 4a and b displays scanning electron micrographs of samples calcined at 880 °C. Values of the granulometrical analyses are given in Table 2. While sample S is a mixture of spherical and edgy particles with a wide particle size distribution, sample SG comprises more spherical particles with a narrower size distribution. As also shown in Table 2, sample SG shows lower tetragonality. We therefore tried to examine factors dominating particle size distribution and tetragonality. Figure 5 displays the backscattered electron images of SEM. The aspect ratio and particle size of the needle like $BaCO_3$ particle are smaller in sample SG without severe agglomeration, in spite of intensive milling.

Microstructural difference in the samples S and SG upon heating is now discussed on the basis of STEM and SEM

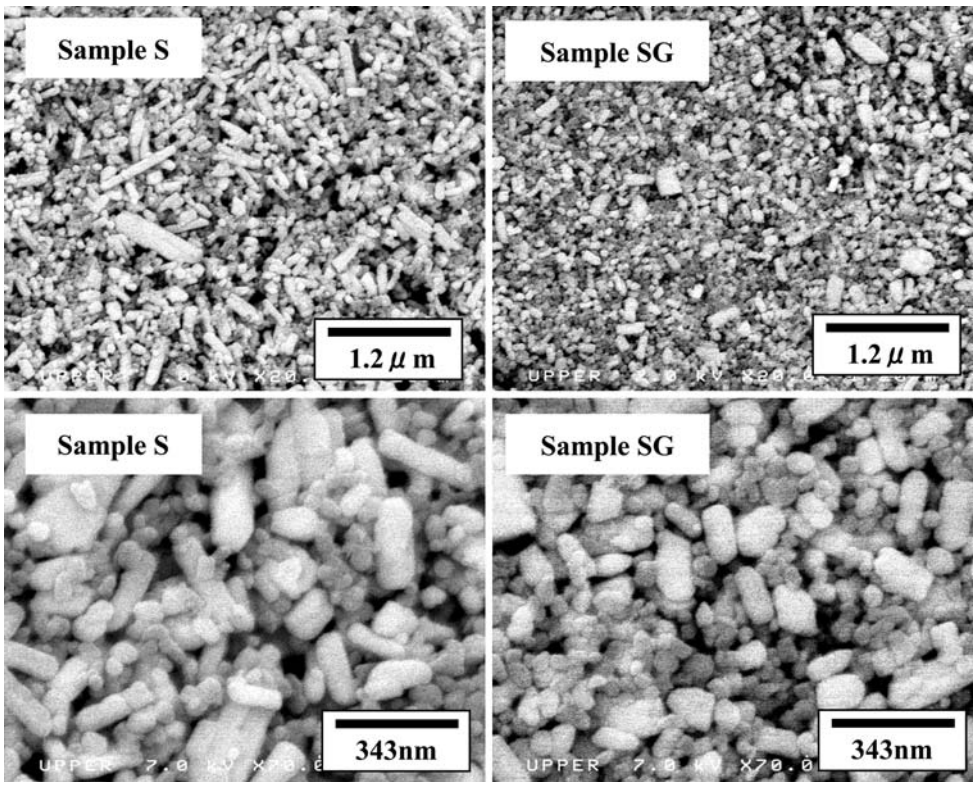

Fig. 5 SEM-BSE micrographs of S and SG mixtures before calcination

micrographs of the samples quenched from 700 and 790 °C. Figure 6a and b exhibits two distinct particulate species, i.e. large ones above 100 nm and agglomerated ones of about 50 nm with very fine primary particles. We have confirmed by energy dispersive analysis that these larger ones are $BaCO_3$. We further detected agglomerated TiO_2 surrounded by fine BT particles.

When we increased the heating temperature from 700 to 790 °C, general tendency of the morphological difference remains unchanged, as shown in Fig. 7a and b. Remaining large $BaCO_3$ particles are formed as a consequence of local compositional inhomogeneity, leading to a broader particle size distribution of BT, particularly in the case of sample S. As summarized in Table 3, particle size of sample SG was twice larger than that of sample S at both temperatures. We therefore note that dry milling accelerates not only the BT formation but also BT particle growth simultaneously.

Discussion

Crystallographical properties

Table 4 shows the results of XRD analyses. Sample SG shows broader peaks of all the starting materials. Wakamatsu et al. [22] reported that brookite and rutile were formed by mechanical milling treatment of anatase. Although brookite peak was not detected in XRD profile of sample SG, we observed an increase in the rutile phase with a slight decrease of anatase. This result revealed that the crystalline states of the starting material were degraded by strong mechanical treatment to enhance the reactivity of the starting mixture.

Results of XRD of the samples quenched either from 700 or 790 °C are summarized in Table 5. Sample SG quenched from 700 °C showed the larger lattice volume. This indicates that the BT crystals of sample SG contain larger amount of lattice imperfection. For sample SG, crystallite sizes of the samples quenched from 700 and 790 °C were fairly large, i.e. at the range from 10 to 50 nm. We obtained these values after Rietveld refining secondary profile parameters of Pseudo-Voigt function proposed by Tompson, Cox and Hastings by using RIETAN-2000 [21]. When the particle size determined from the image analysis was divided by the crystallite size, the quotient for samples S and SG were 0.9 and 1.5 for those quenched from 700 °C, and 1.4 and 1.6 for those from 790 °C, respectively. The larger number of the crystallites in a particle for the sample SG suggests higher possibility of coalescence of BT particles without significant growth of crystallites during calcination. A decrease in the reaction initiation temperature without sacrifice of tetragonality was recognized by adding glycine and milled with a vibration mill

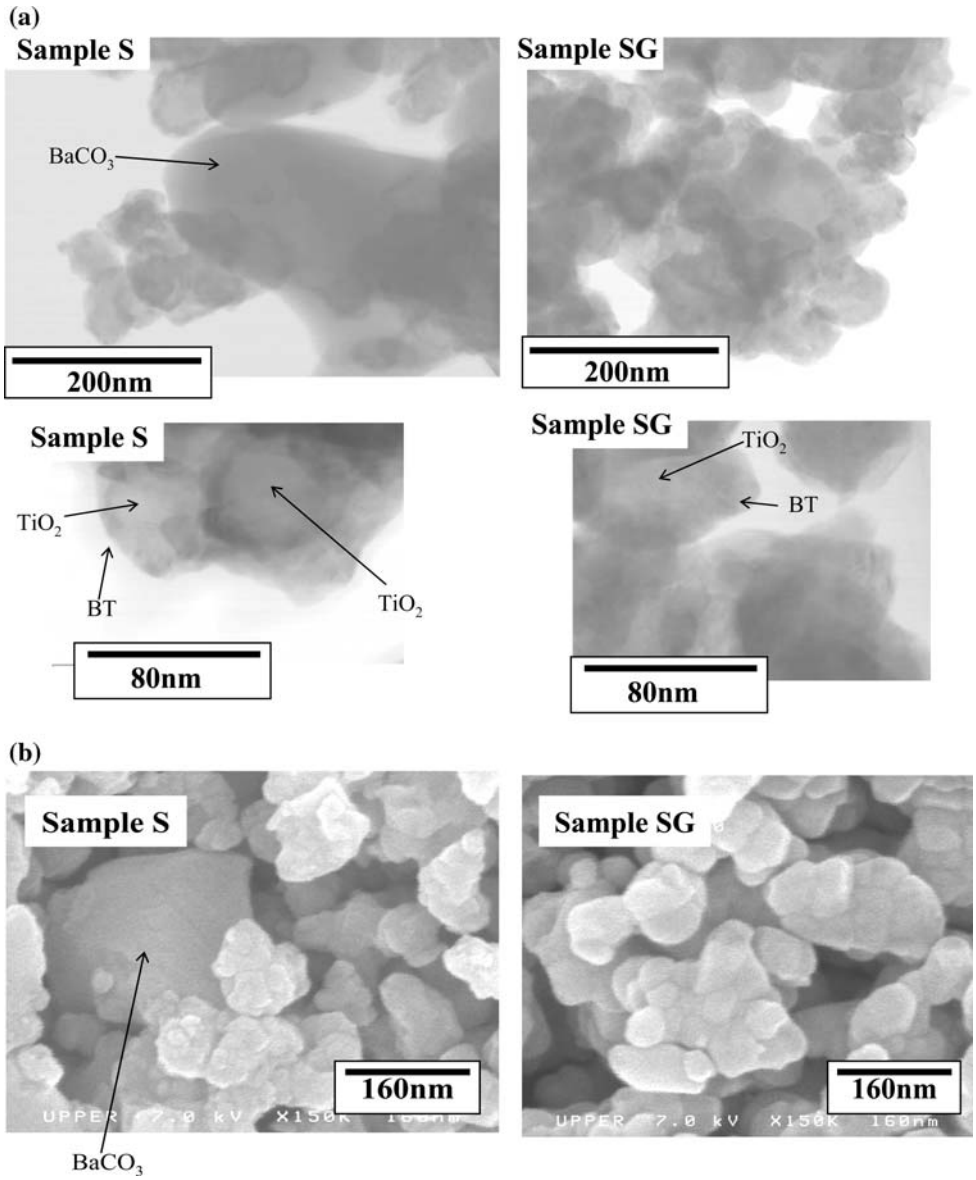

Fig. 6 (**a**) STEM-BF and (**b**) SEM micrographs of samples S and SG quenched from 700 °C

[11, 19], the stress intensity of which was smaller than the present planetary milling. From these results, we attribute the undesirable grain growth for the sample SG to the excessive mechanical stressing by planetary mill, which induces fast diffusion of Ba^{2+} into TiO_2 and, hence, coalescence of BT particles.

As discussed above, dry ball milling with the organic additives is effective to obtain BT particle of narrow particle size distribution. Dry milling disintegrates $BaCO_3$ particles and improves mixing homogeneity. BT formation is completed at lower temperatures before grain growth of unreacted starting material occurs due to highly active surface and presence of organic additives. However, the highly active surface of staring mixture caused to form BT particles with lower crystallinity and, hence, lower tetragonality. Achievement of homogenization under severe mechanical stressing is, therefore, not always appropriate for the purpose of synthesizing BT microparticles, in spite of attaining high homogeneity of the starting mixture to a significant extent.

Mixtures prepared from finest starting powders with less mechanical stress

From the experimental results given above, it turned out to be necessary to increase homogeneity of the starting mixture without exerting severe mechanical stressing. We therefore prepared an alternative starting mixture, i.e. sample FB, using ultra-fine starting materials by homogenizing in a slow-rotating pot mill. Figure 8 shows the SEM-BSE micrograph of sample FB, which exhibits much finer particles.

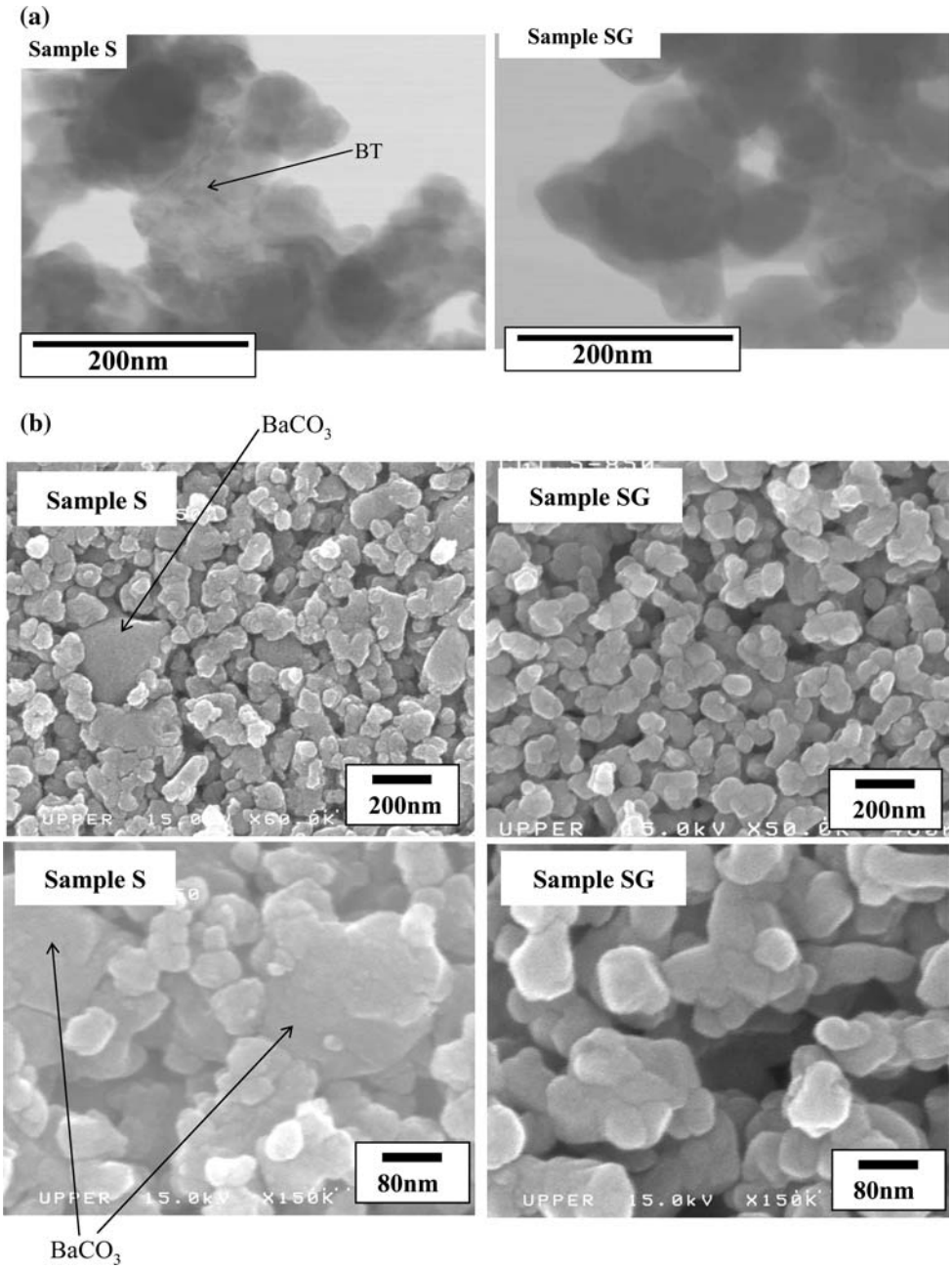

Fig. 7 (**a**) STEM-BF and (**b**) SEM micrographs of samples S and SG quenched from 790 °C

Table 3 SBET and average BT particle size of quenched samples

Sample	700 °C		790 °C	
	SBET (m^2/g)	BT particle size (nm)	SBET (m^2/g)	BT particle size (nm)
S	13.4	15	12.5	33
SG	11.6	28	8.6	75
FB	32.4	18	19.5	47

The DTG curves of sample FB and SG are shown in Fig. 9. Sample FB exhibits the fraction of the first step weight loss much larger than S and SG with simultaneous decrease of the reaction termination temperature. Figure 4c and Table 2 demonstrate finer particulates with narrower size distribution of calcined FB.

Electron micrographs of sample FB during processing are displayed in Fig. 10. Results of particle size analysis

Table 4 Crystallinity of mixture samples determined by XRD

Sample	FWHM (°)			Rutile (%)
	$BaCO_3$ (111)	Anatase (101)	Rutile (101)	
S	0.238	0.236	0.217	39
SG	0.256	0.239	0.239	41

based on Fig. 10 are summarized in Table 3. There were not large $BaCO_3$ particles in samples FB and SG. Decrease in the reaction temperature of sample SG by mechanical activation with glycine obviously suppressed grain growth of the reactant, $BaCO_3$. This accords with the sharper particle size distribution as shown in Fig. 4c. Figure 11 shows the relationship between the median particle size of BT quenched from 700 and 790 °C and the crystallite size. Sharper size distribution and smaller average particle size of those from sample FB is quite obvious, as shown in Fig. 4c. Single particle of BT born from sample FB is close to single crystallite and hence its crystallinity is correspondingly higher. This closes up the benefits of sample FB to obtain well-crystallized products formed.

Finally, values of the tetragonality of BT are compared in Table 2. At a sight, the difference in the particle size and tetragonality of the samples calcined at 880 °C does not seem too much. However, when we look at Fig. 12, where the tetragonality is plotted as a function of the average particle size, the difference becomes appreciable. The curve of BT derived from sample FB is located upper left, showing that the tetragonality is higher than any other samples while keeping small particle size. When we compare the particle size at tetragonality 1.0080, the average particle sizes are 116 and 122 nm for samples FB and S, respectively. The tetragonality values at particle size 120 nm are 1.0082 and 1.0078 for samples FB and S, respectively.

Wada [5] synthesized BT by calcining the BT crystal powder obtained by a hydrolysis method. He obtained 200 nm BT particles with high tetragonality and claimed merits of starting from smaller particles. Their success might be attributed to the elimination of lattice defects from desorption of OH groups by heat treatment due to rapid growth within a small particles, i.e. shorter distance of defects migration in minute particles, enabling easier defect extinction.

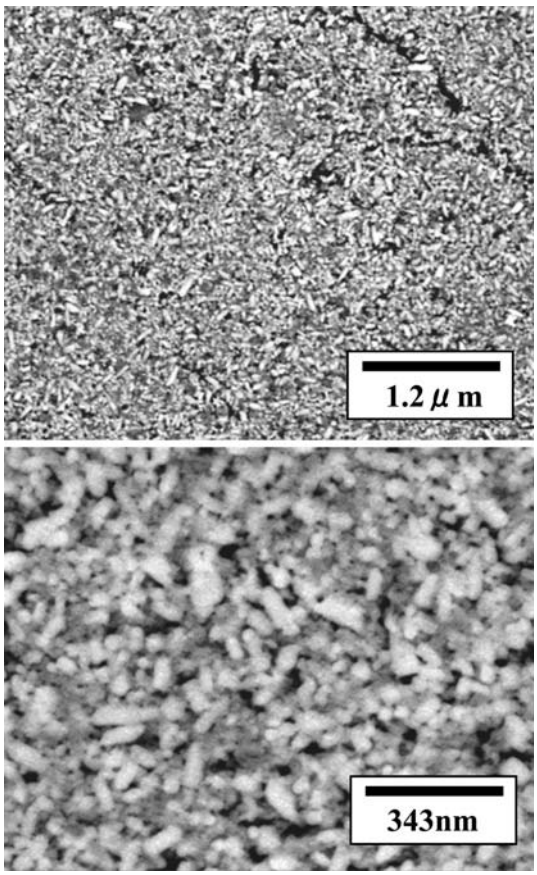

Fig. 8 SEM-BSE micrographs of FB mixture before calcination

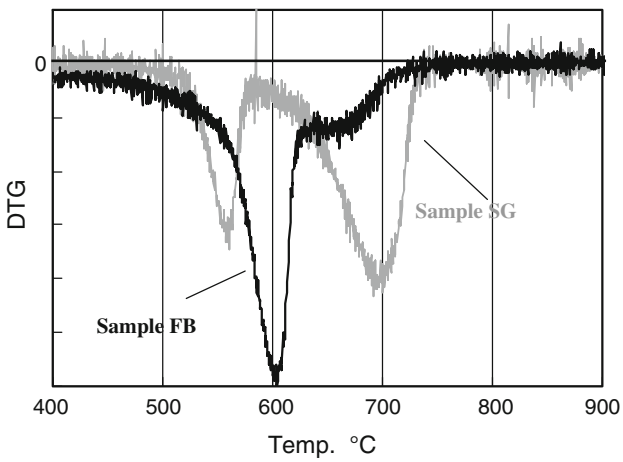

Fig. 9 DTG profile of the samples FB and SG

Table 5 Crystallinity of BT quenched from 700 and 790 °C

Sample	700 °C			790 °C		
	FWHM (111) (°)	Crystallite size (nm)	Lattice volume (Å^3)	FWHM (111) (°)	Crystallite size (nm)	Lattice volume (Å^3)
S	0.632	15.8	64.86	0.437	23.8	64.76
SG	0.582	18.8	64.93	0.265	45.9	64.56
FB	0.538	19.4	64.87	0.294	37.2	64.59

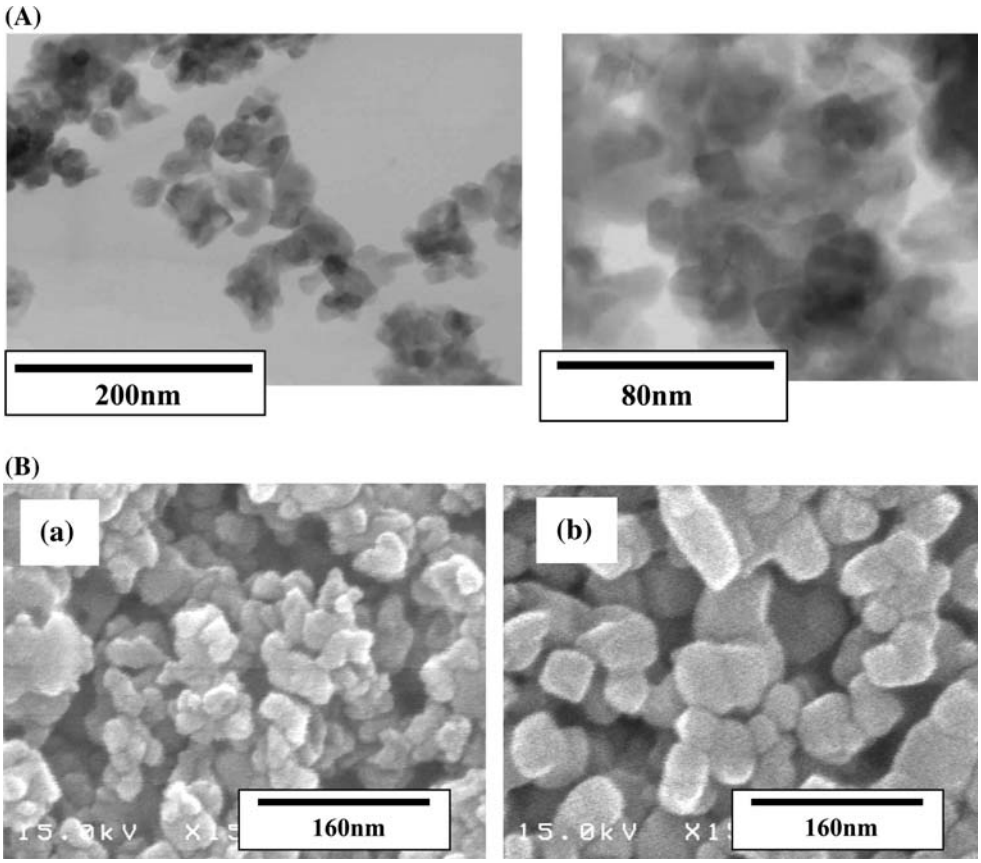

Fig. 10 (**A**) STEM-BF micrographs of sample FB quenched from 700 °C. (**B**) SEM micrographs of samples FB quenched from (a) 700 °C and (b) 790 °C

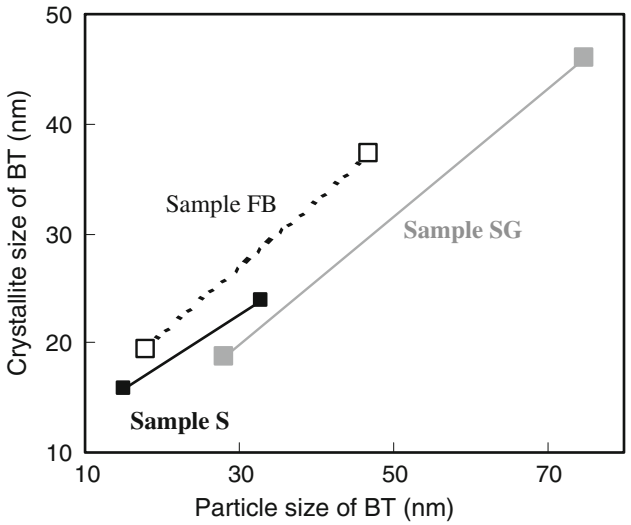

Fig. 11 Crystallite size of BT quenched from 700 and 790 °C as function of the particle size

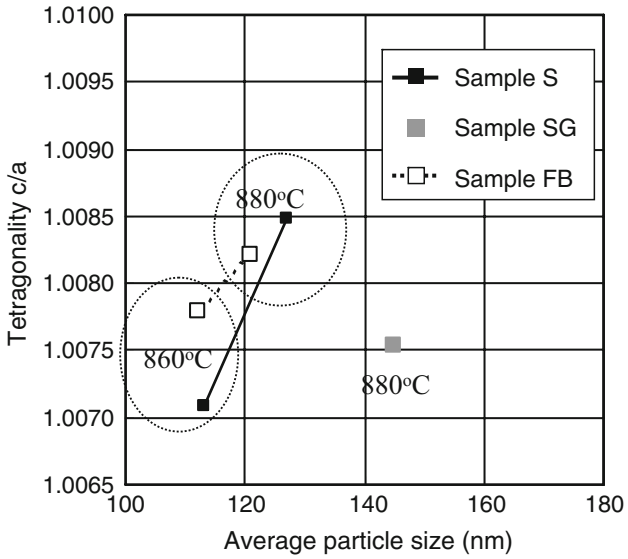

Fig. 12 Relationship between tetragonality and particle size of BT calcined at 860 and 880 °C

As shown in Table 5 and Fig. 11, BT particles from SG are larger than those from S or FB. They are actually agglomerates of smaller crystallites and contain highly concentrated defect density. This explains low tetragonality of BT from sample SG, in accordance with the report of Wada [5]. Particle size of BT via a solid state route is known to reflect that of TiO_2 [14]. As we confirmed in our present study as well as the previous report [8], BT particles much finer than that of TiO_2 are formed at the beginning of their formation and are growing up to the size closer to that of TiO_2 particles. When the starting TiO_2 is

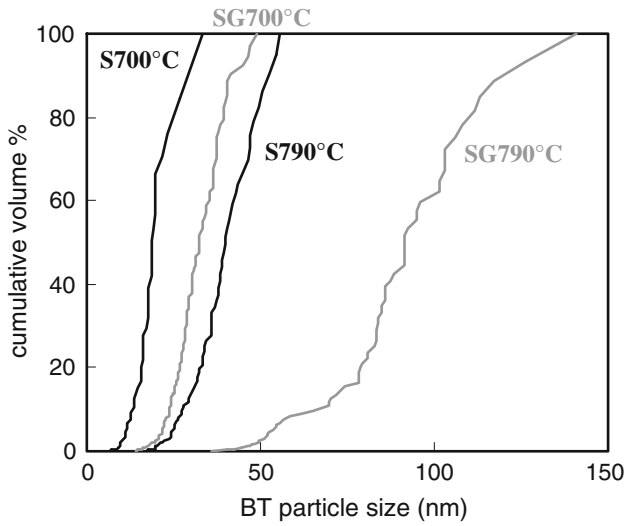

Fig. 13 Particle size distribution of BT primary particle of quenched samples

aggregated, the final particles of the product BT are also aggregated or coalesced, and hence correspondingly larger. Fujikawa et al. [15] reported similar observation. Larger BT particles were formed from sample SG than from S in the present study. The states of agglomeration of TiO_2 in sample SG are not clearly visible in Fig. 5. From Fig. 6, however, we recognize higher degree of agglomeration and hence larger aggregates of TiO_2 particles with their surface densely covered by tinier BT particles.

When we activate the starting mixture in an attempt to expedite the reaction, larger number of BT crystallites are formed quickly. From the process described above, it is reasonably anticipated that the increase in the BT particle size is predominated by coalescence. The particle size distribution curves of BT primary particle quenched from 700 and 790 °C are shown in Fig. 13. The average particle size of BT from sample SG quenched from 790 °C is larger than that of the starting TiO_2. It is also to be noted that the distribution curve is discontinuous. These observations favor coalescence mechanism to mere particle growth rather than crystallite growth, with the participation of the behavior as agglomerated TiO_2.

When we started from sample FB, in contrast, we obtained BT with higher tetragonality and smaller particle size, as shown in Fig. 12. Here we paid efforts to use TiO_2 particles smaller than those of BT particles observed at temperatures as low as 700 °C, suppressing unnecessary surface activation by adopting a mixing procedure under lowest possible mechanical stress. This was obviously successful to suppress coalescence, resulting in the smaller particles with high tetragonality, c/a. It is thus obvious that sample FB leads to BT particles with their properties closest to our goal.

Summary

Growth processes of crystallites and particles of BT during the early stages of BT formation via a solid state route were compared by using three different starting mixtures with widely different reactivity. Addition of glycine and simultaneous intensive mechanical activation turned out to be very effective to elevate the reactivity and hence decreasing the reaction temperature. This was accompanied, however, by undesirable decrease in the tetragonality and increase in the particle size. As we suppressed the mechanical stressing and tried to mix finer starting materials as homogeneously as possible, we obtained finer BT particles with higher tetragonality. From these observations we conclude that suppression of (i) the grain growth of the unreacted $BaCO_3$ and (ii) growth of BT by coalescence lead to finer BT particles with sharper particle size distribution and higher tetragonality. Intensive mechanical stressing and insufficient dispersion of TiO_2 are to be avoided. When these conditions are fulfilled, well crystallized BT of 116 nm with its tetragonality as high as 1.0078 is attained via a solid state process.

Acknowledgement The authors are thankful to Mr. T. Hagiwara for Rietveld analysis.

References

1. Mizuno Y, Hagiwara T, Kishi H (2007) J Ceram Soc Jpn 115:360. doi:10.2109/jcersj.115.360
2. Arlt G, Hennings D, With G (1985) J Appl Phys 58:1619. doi:10.1063/1.336051
3. Dawson WJ (1988) Am Ceram Soc Bull 67:1673
4. Hennings D, Rosenstein G, Schreinemacher H (1991) J Eur Ceram Soc 8:107. doi:10.1016/0955-2219(91)90116-H
5. Wada N (2004) J Soc Powder Technol Jpn 41:35
6. Hennings DFK, Schreinemacher BS, Schreinemacher H (2001) J Am Ceram Soc 84:2777
7. Buscaglia MT, Bassoli M, Buscaglia V, Alessio R (2005) J Am Ceram Soc 88:2374. doi:10.1111/j.1551-2916.2005.00451.x
8. Ando C, Yanagawa R, Chazono H, Kishi H, Senna M (2004) J Mater Res 19:3592. doi:10.1557/JMR.2004.0461
9. Yanagawa R, Sennna M, Ando C, Chazono H, Kishi H (2007) J Am Ceram Soc 90:809. doi:10.1111/j.1551-2916.2007.01498.x
10. Ando C, Chazono H, Kishi H (2004) Key Eng Mater 269:161
11. Oguchi H, Ando C, Chazono H, Kishi H, Senna M (2005) J Phys France IV 128:33
12. Ando C, Kishi H, Oguchi H, Senna M (2006) J Am Ceram Soc 89:1709. doi:10.1111/j.1551-2916.2006.00917.x
13. Kubo T, Kato M, Fujita T (1967) Kogyo Kagaku Zasshi 70:847
14. Niepce JC, Thomas G (1990) Solid State Ionics 43:69. doi:10.1016/0167-2738(90)90472-4
15. Fujikawa Y, Yamane F, Nomura T (2003) J Jpn Soc Powder Metall 50:751
16. Lotnyk A, Senz S, Hesse D (2006) Solid State Ionics 177:429. doi:10.1016/j.ssi.2005.12.027
17. Lotnyk A, Senz S, Hesse D (2007) Acta Mater 55:2671. doi:10.1016/j.actamat.2006.12.022

18. (a) Senna M (1993) Solid State Ionics 3:63; (b) Senna M (2001) Mater Sci Eng A 39:304; (c) Senna M (2002) Ann Chim Sci Mat 27:3
19. Ando C, Tsuzuku K, Kobayashi T, Kishi H, Kuroda S, Senna MJ, Mater Sci: Mater Electron (to appear)
20. Society of Powder Technology (1994) Particle size analysis and technology. Nikkan-Kogyo Shinbun shya, Tokyo
21. Izumi F, Ikeda T (2000) Mater Sci Forum 321–324:198
22. Wakamatsu T, Fujiwara T, Ishihara KN, Shingu PH (2003) J Jpn Soc Powder Metall 48:950